

Some New Perspectives of Utilizing TOF Information for Improving PET Imaging

Chien-Min Kao
Assistant Professor
Department of Radiology
The University of Chicago



Introduction & Motivation

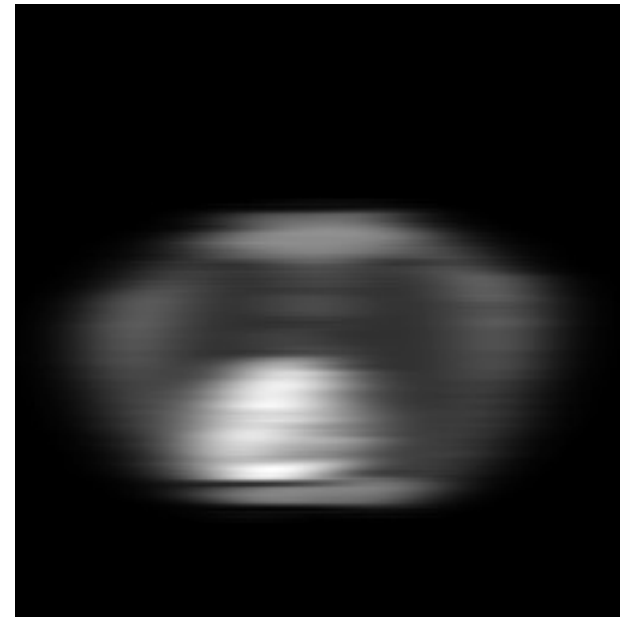
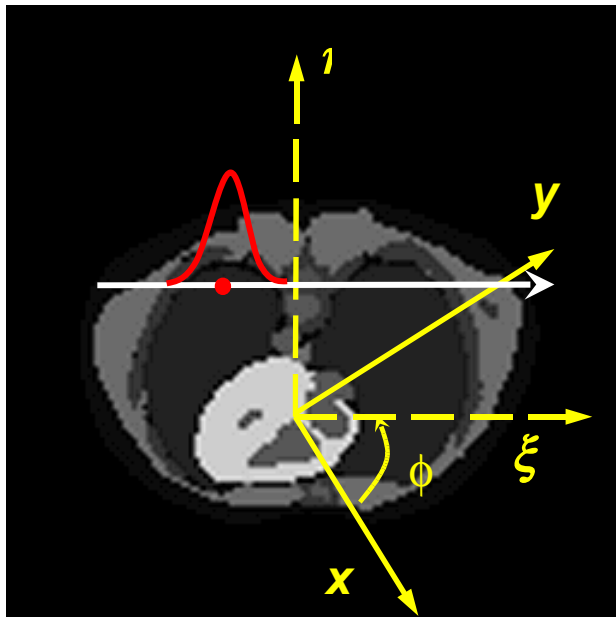
- TOF measurement is known to yield improved image SNR:

$$SNR_{gain}^2 \propto D / \sigma$$

- Timing resolution has improved substantially.
- Redundancy in TOF-PET data suggests image reconstruction can be achieved by multiple ways of utilizing data (MIC06 & 07).
 - Can TOF information help rejection of scatter or random events?



2D TOF-PET model



$$p_\phi(\xi, \eta) = \int_{-\infty}^{\infty} d\eta \ f(\xi \hat{\phi} + \eta \hat{\phi}_\perp) h_\sigma(\eta) \quad h_\sigma(x) = \frac{1}{\sqrt{2\pi}\sigma} e^{-x^2/2\sigma^2}$$

Data redundancy

$$p_\phi(\xi, 0) h_\sigma(\xi) = \int d^2x \{f(x)h_\sigma(x)\} \delta(\xi - x \cdot \hat{\phi})$$

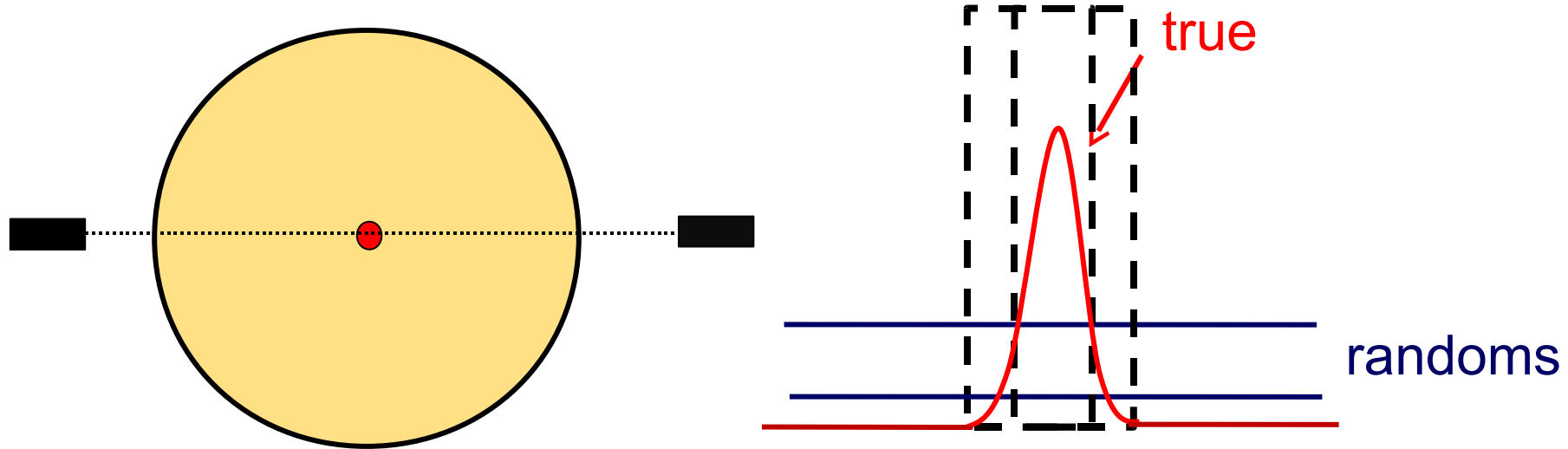
$$h_\sigma(\vec{x}) = \frac{1}{\sqrt{2\pi}\sigma} e^{-|\vec{x}|^2/2\sigma^2}$$

$$p_\phi(\xi, 0) \Rightarrow f(x)h_\sigma(x)$$

infinitesimal coincidence window

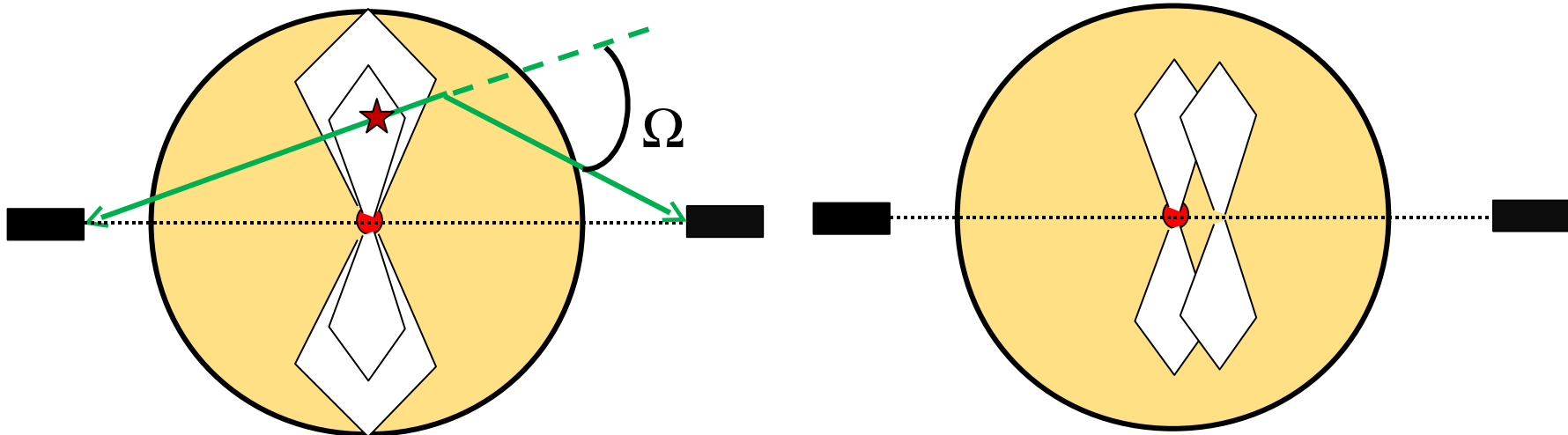


Reject background events



Adjusting coincidence window may improve rejection of scatter and randoms with respect to a point of interest.

Scatter rejection

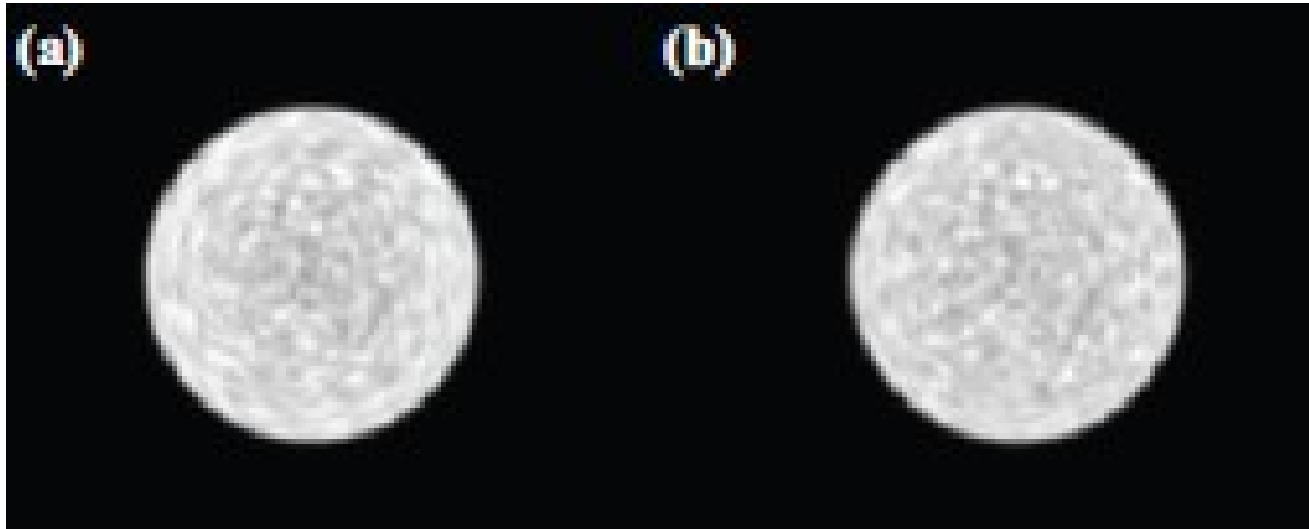


Effects of energy
resolution and
energy window

Effects of timing
resolution



Finite-CW reconstruction



600ps CW

1ns CW

40 cm (~1.3 ns) diameter, 16.2 cm height cylinder
82.5 cm-diameter 2D PET, 6.45x6.45x25mm³ LSO
300 ps FWHM timing res. And 30% energy res.



Finite-CW reconstruction (cont'd)

CW	600ps		1 ns		1.4 ns		2ns	
system	1	2	1	2	1	2	1	2
SF	25.4%	19.7%	26.7%	20.2%	27.4%	20.6%	27.6%	20.8%
RF	8.6%	6.8%	10.4%	7.8%	12.9%	9.4%	17.3%	12.4%
NECR (x10)	0.831	0.737	1.056	1.001	1.100	1.099	1.053	1.095
SNR gain (EM reconstruction)								
T	1.84	1.62	1.86	1.63	1.88	1.67	1.87	1.59
T+S	1.82	1.47	1.81	1.46	1.76	1.47	1.79	1.43
T+R	2.28	1.74	2.17	1.73	2.17	1.76	2.23	1.67
T+S+R	2.35	1.74	2.40	1.77	2.36	1.82	2.39	1.75

system 1: Er=30%, Tr=300ps; system 2: Er=10%, Tr=700ps



Windowed Reconstruction

$$q_{\phi}^{(\omega)}(\xi) = \Re \left\{ f(\vec{x}) \varphi^{(\omega)}(\vec{x}) \right\}$$

$$q_{\phi}^{(\omega)}(\xi) = \int \int d^2 x_s h_{\sigma}(\xi - x_s \cdot \hat{\phi}) \omega(x_s) p_{\phi}(\xi, x_s \cdot \hat{\phi}_{\perp})$$

$$\varphi^{(\omega)}(x) = \int \int d^2 x_s \omega(x_s) h_{\sigma}(x - x_s)$$

$$\begin{aligned} f(\vec{x}) \varphi^{(\omega)}(\vec{x}) &= \int d\phi \int d\xi k(\vec{x} \cdot \hat{\phi} - \xi) q_{\phi}^{(\omega)}(\xi) \xleftarrow{\text{FBP}} \\ &= \int d\phi \int d\xi k(\vec{x} \cdot \hat{\phi} - \xi) \int d\eta \varpi_{\phi}(\xi, \eta) p_{\phi}(\xi, \eta) \end{aligned}$$

TOF data window

$$\varpi_{\phi}(\xi, \eta) = \int d\xi' h_{\sigma}(\xi - \xi') \omega_{\phi}(\xi', \eta), \omega_{\phi}(\xi, \eta) = \omega(\xi \hat{\phi} + \eta \hat{\phi}_{\perp})$$



Special cases

$$\vec{f}(x) = \frac{\sigma_r}{\sigma_e} \int_0^\pi d\phi (e^{-\eta^2/2\sigma_r^2} e^{-\xi^2/2\sigma_e^2} k(\xi)) \otimes p_\phi(\xi, \eta)$$

$$\sigma_e^2 = \sigma^2 + \sigma_r^2$$

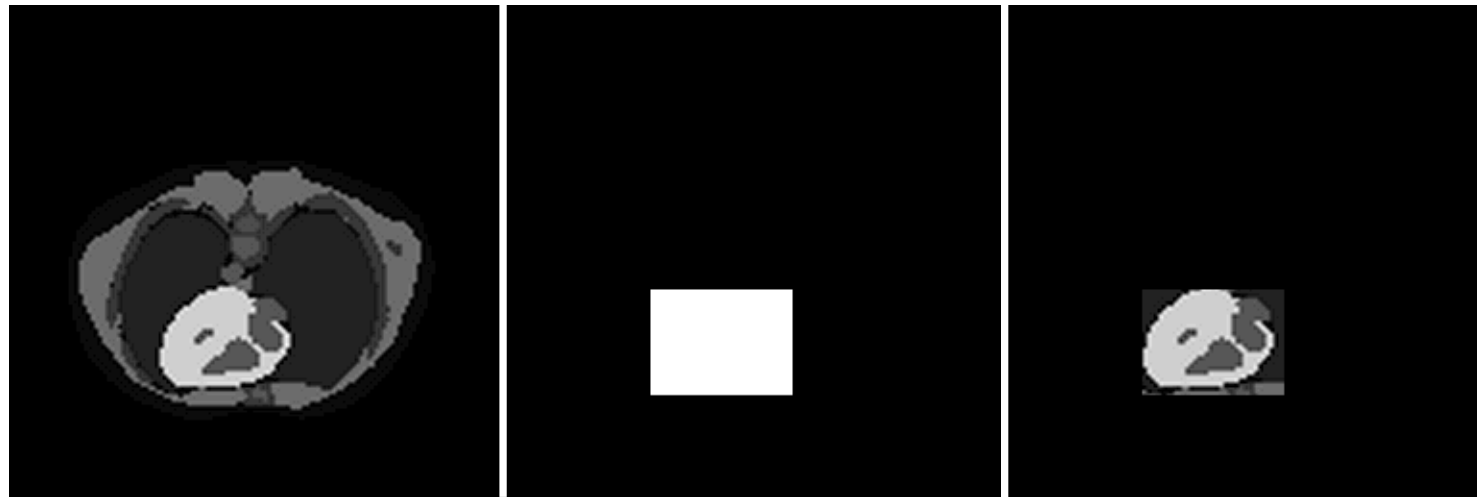
$$(1) \sigma_r = \sigma : f(x) = \frac{1}{\sqrt{2}} \int_0^\pi d\phi (e^{-\eta^2/2\sigma^2} e^{-\xi^2/4\sigma^2} k(\xi)) \otimes_{\xi, \eta} p_\phi(\xi, \eta) \Big|_{\begin{array}{l} \xi = \vec{x} \cdot \hat{\phi} \\ \eta = x \cdot \hat{\phi}_\perp \end{array}}$$

CRG-CW algorithm

$$(2) \sigma_r \rightarrow 0 : f(x) = \sqrt{2\pi} \sigma \int_0^\pi d\phi (e^{-\xi^2/2\sigma^2} k(\xi)) \otimes_\xi p_\phi(\xi, \eta) \Big|_{\begin{array}{l} \xi = \vec{x} \cdot \hat{\phi} \\ \eta = x \cdot \hat{\phi}_\perp \end{array}}$$



Example



image

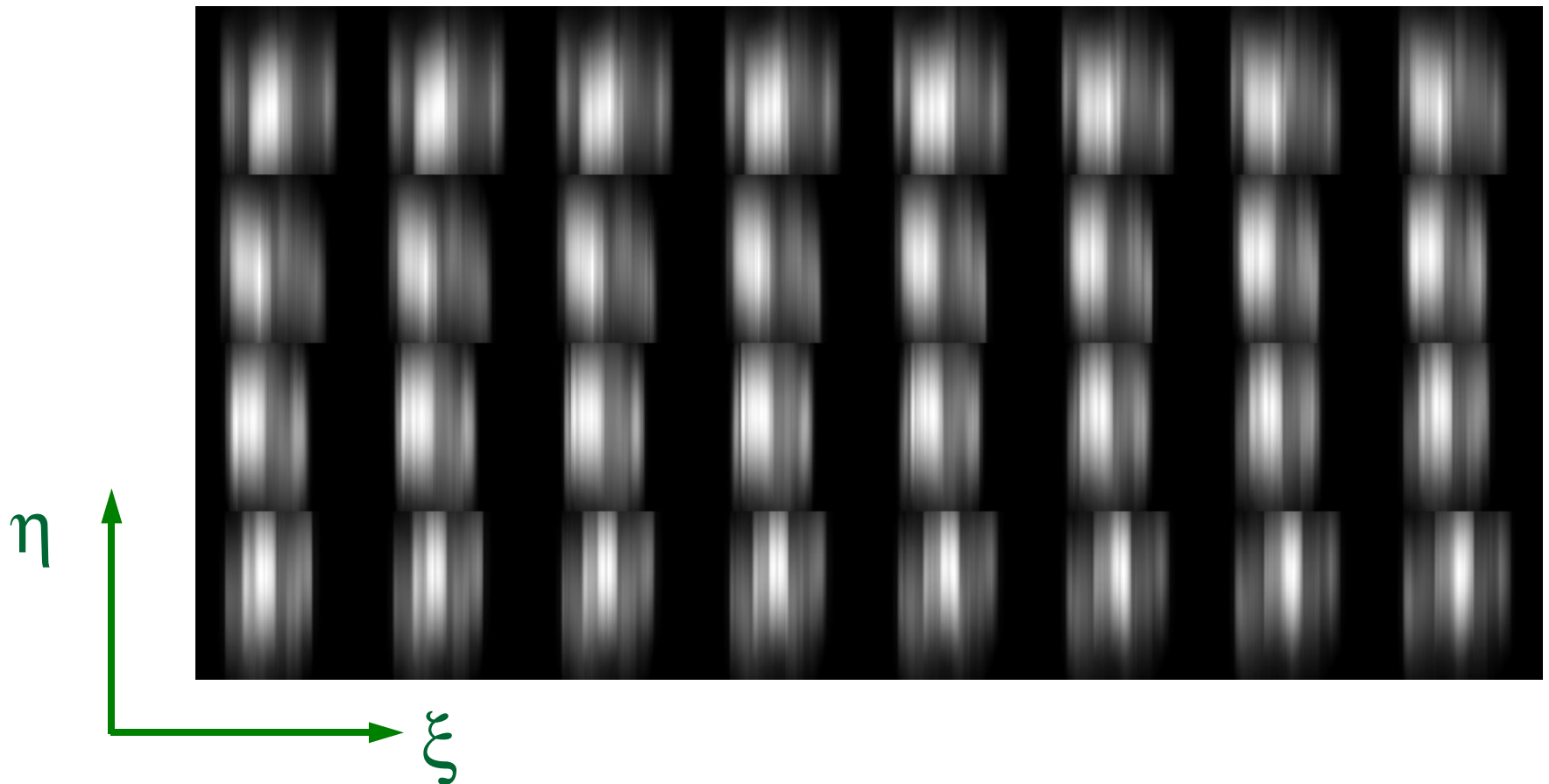
ROI

ROI Image



TOF-PET data

2ns FWHM



Reconstruction

2ns FWHM



$f(\vec{x})\varphi^{(\omega)}(\vec{x})$

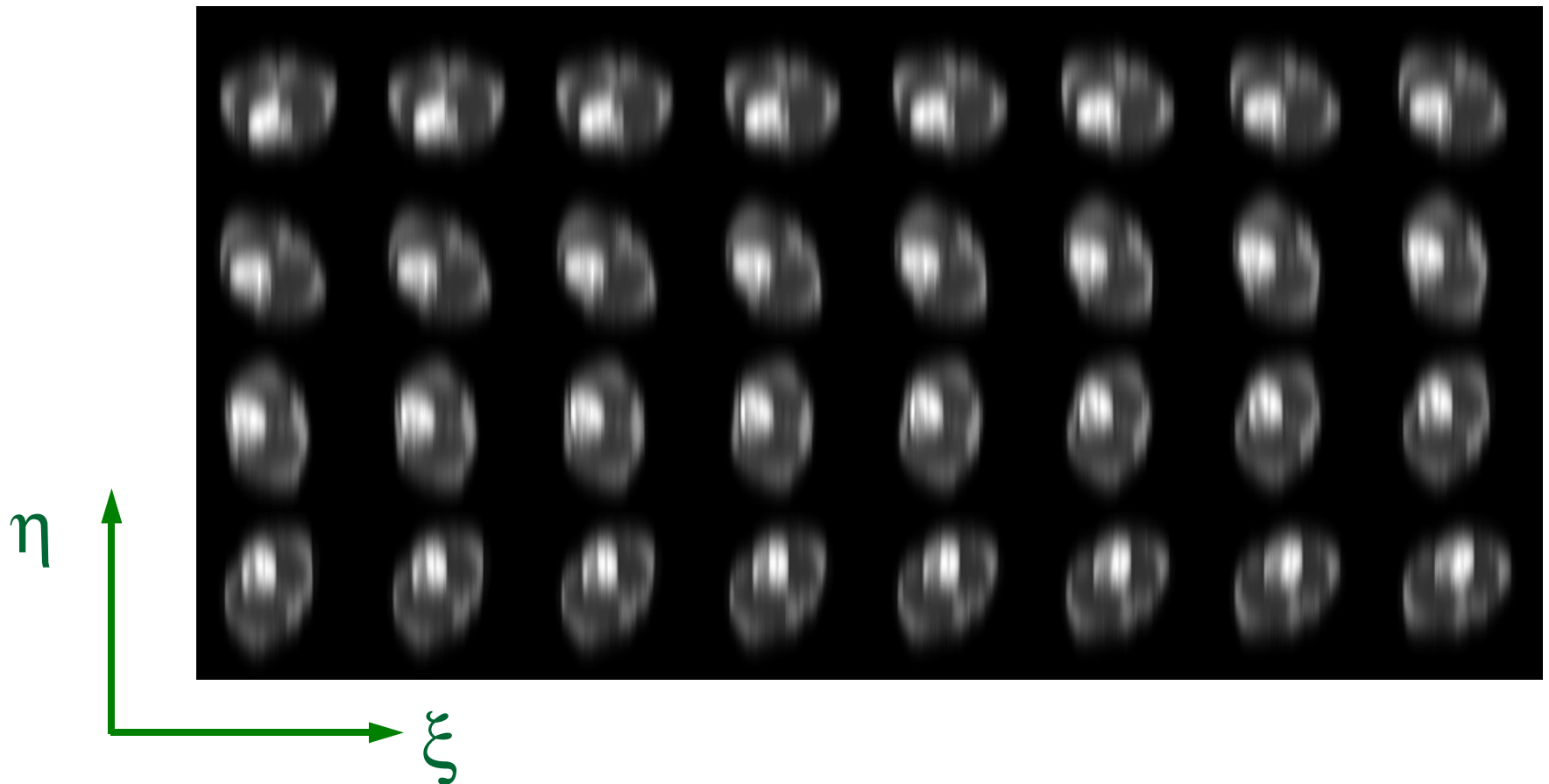
$f(\vec{x})$

true



TOF-PET data

600ps FWHM



Reconstruction

600ps FWHM



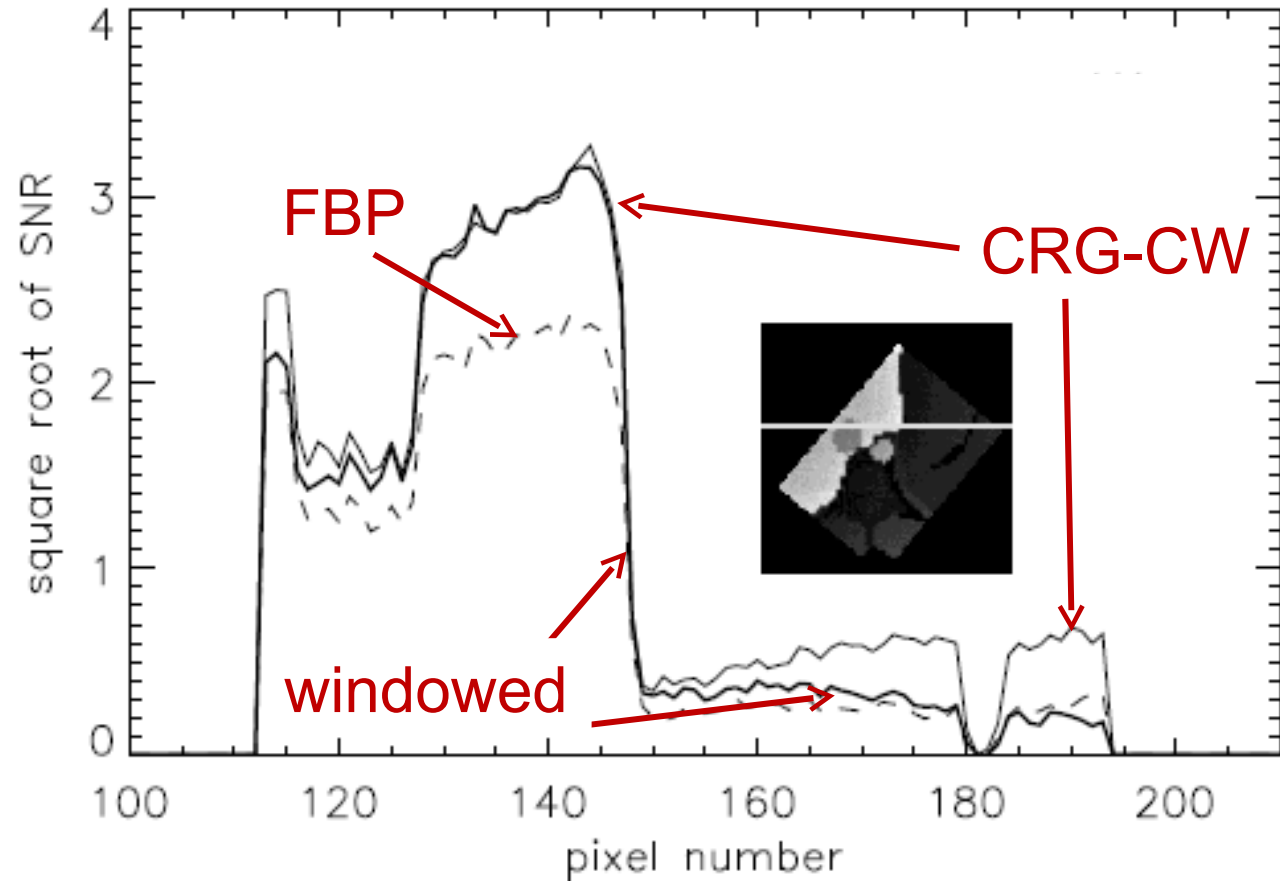
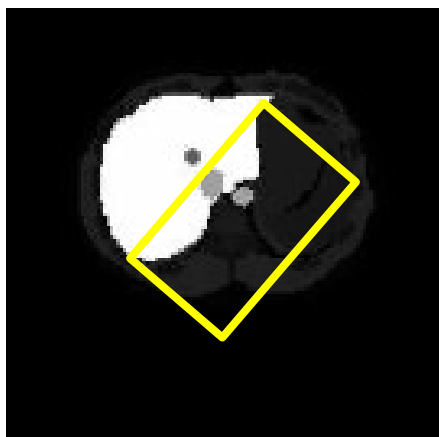
$f(\vec{x})\varphi^{(\omega)}(\vec{x})$

$f(\vec{x})$

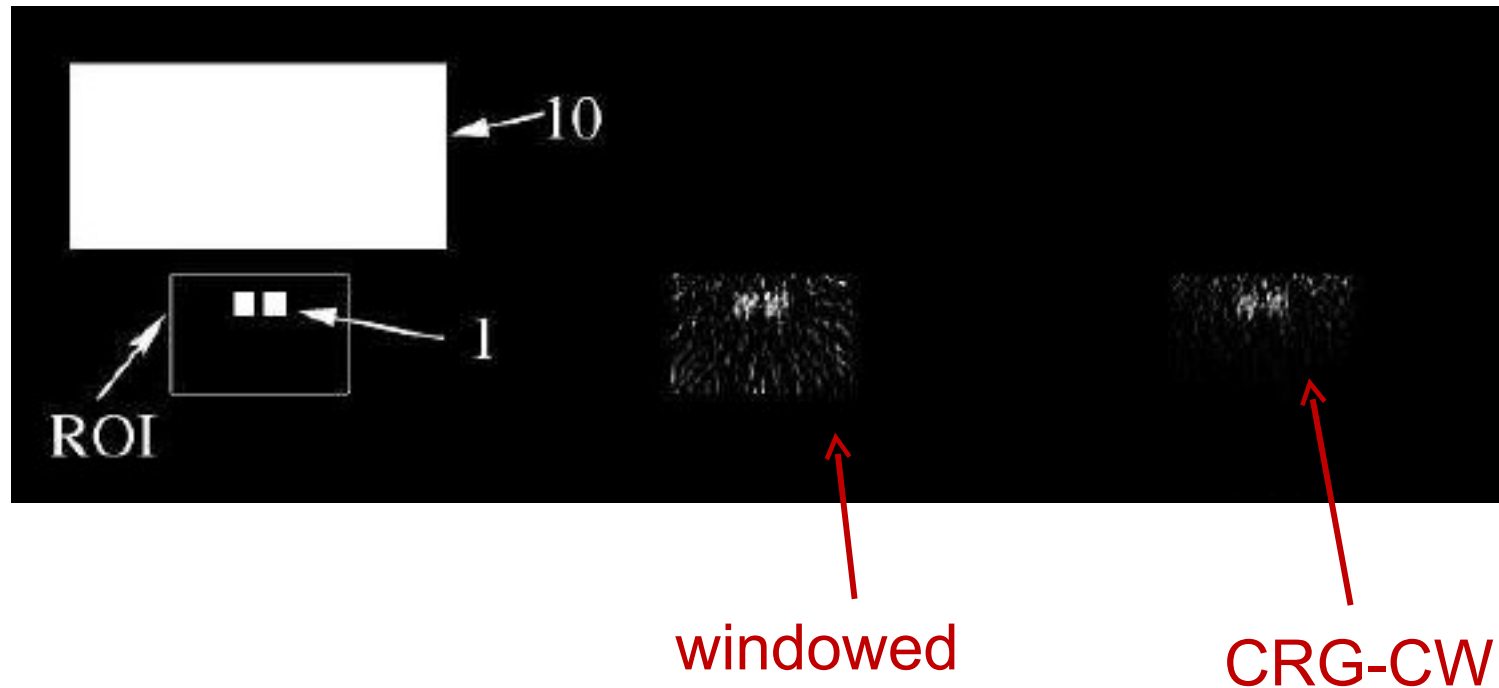
true



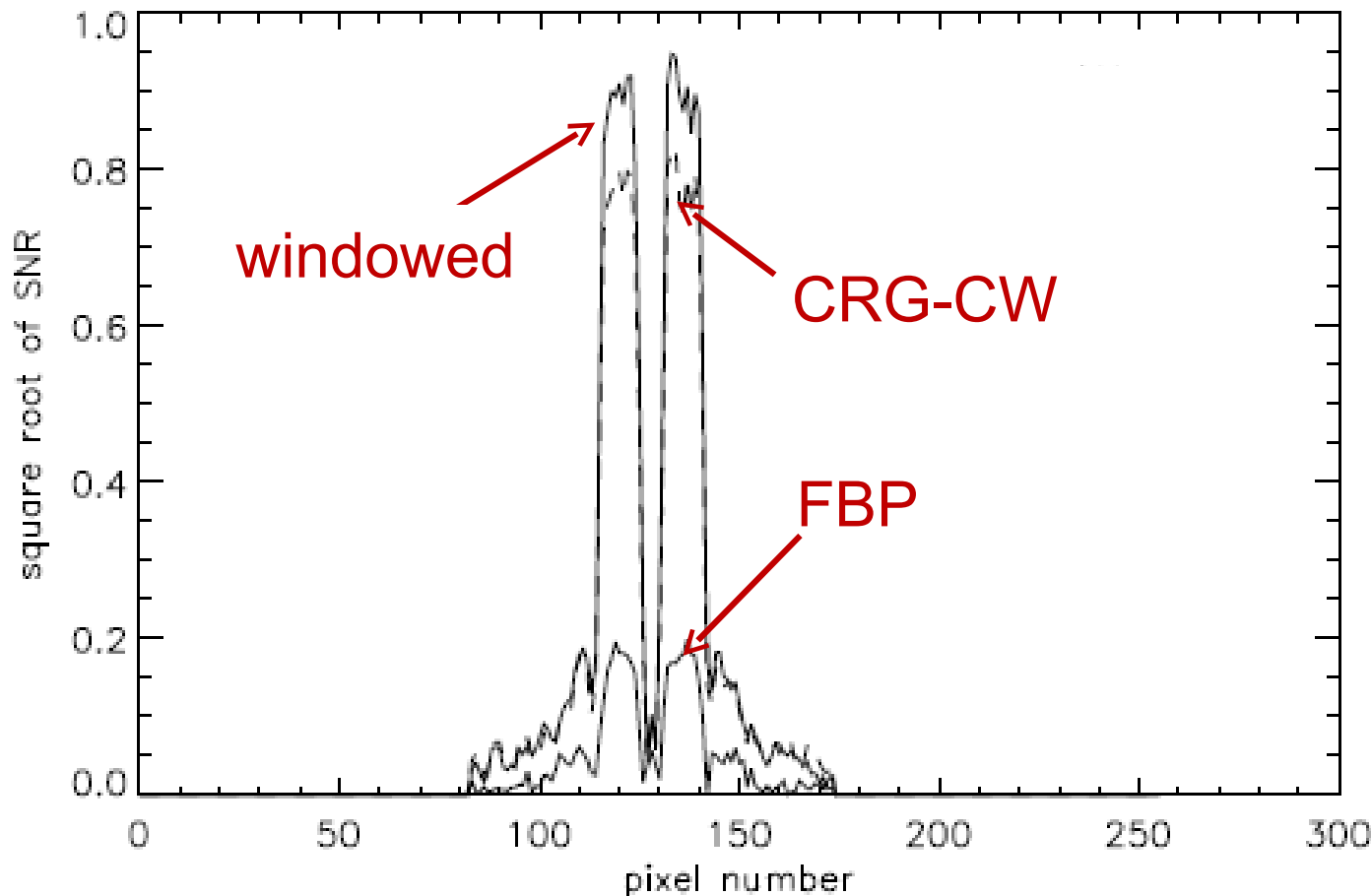
Evaluation I



Evaluation II



Evaluation II (cont'd)



Adaptive to local data statistics

$$\omega_{\vec{x}_0}(\vec{x}) = \operatorname{argmin}_{\omega(\vec{x})} \operatorname{Var}\{\hat{f}^{(\omega)}(\vec{x}_0)\} \text{ subject to } \psi^{(\omega)}(\vec{x}_0) = 1.$$

Solution:

$$\tilde{\omega}_{\vec{x}_0}(\vec{x}) = \int_0^\pi d\phi \int_{-\infty}^\infty d\eta k(\vec{x} \cdot \hat{\phi}_\perp - \eta) \frac{\sigma_\phi^{-2}(\vec{x}_0 \cdot \hat{\phi}, \eta) h_\sigma^2(\vec{x}_0 \cdot \hat{\phi}_\perp - \eta)}{\int_{-\infty}^\infty d\eta \sigma_\phi^{-2}(\vec{x}_0 \cdot \hat{\phi}, \eta) h_\sigma^2(\vec{x}_0 \cdot \hat{\phi}_\perp - \eta)}$$

$$\tilde{\omega}_{\vec{x}_0}(\vec{x}) = h_\sigma(\vec{x}_0 - \vec{x}) \omega_{\vec{x}_0}(\vec{x})$$

$$\operatorname{Var}\{\hat{f}^{(\omega_{\vec{x}_0})}(\vec{x}_0)\} \approx \alpha \int_0^\pi d\phi \left[\int_{-\infty}^\infty d\eta \sigma_\phi^{-2}(\vec{x}_0 \cdot \hat{\phi}, \eta) h_\sigma^2(\vec{x}_0 \cdot \hat{\phi}_\perp - \eta) \right]^{-1}$$

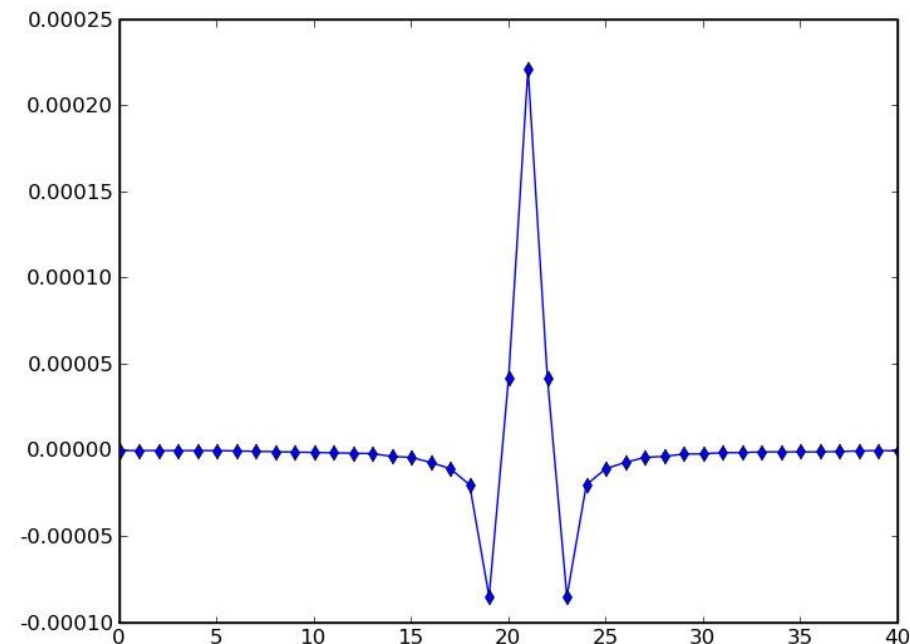
When $\sigma_\phi^{-2}(\xi, \eta)$ is smooth with respect to $h_\sigma^2(\eta)$, it becomes the CRG-CW algorithm (strong assumption).



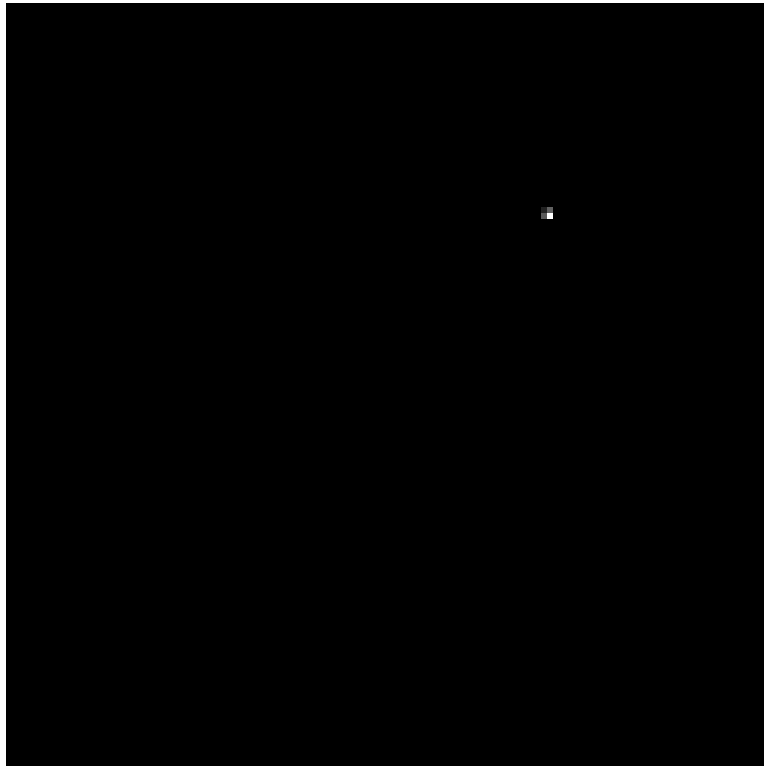
“Real-time” imaging?

$$f(x) = \sqrt{2\pi} \int_0^\pi d\phi \tilde{k}(\xi) \otimes_\xi p_\phi(\xi \eta) \Big|_{\begin{array}{l} \xi \rightarrow x \cdot \hat{\phi} \\ \eta \rightarrow x \cdot \hat{\phi}_\perp \end{array}}$$

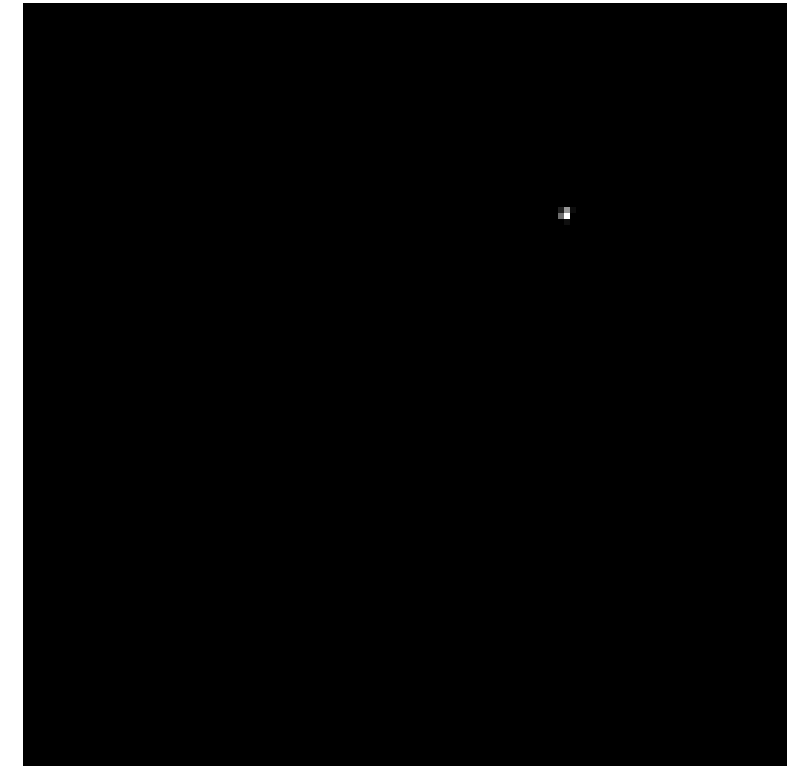
$$\tilde{k}(\xi) = e^{-\xi^2/2\sigma^2} k(\xi)$$



“Real-time” imaging? (600ps FWHM)



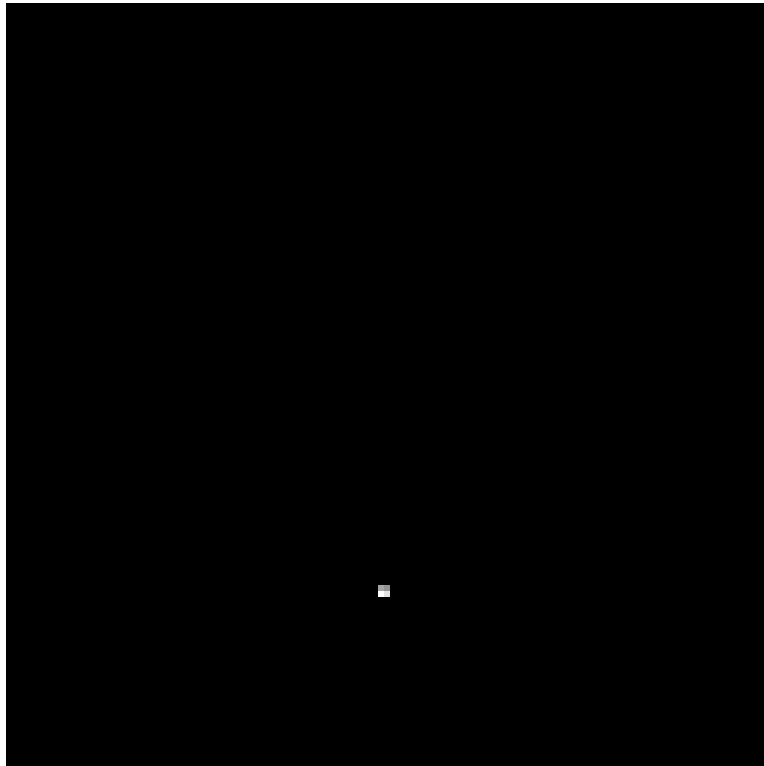
back project



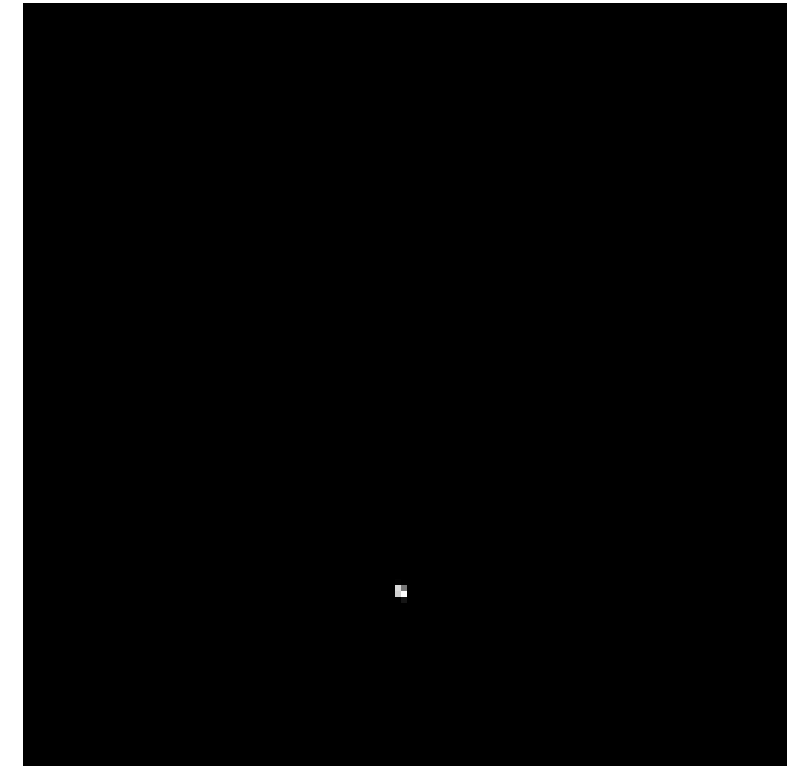
back project with $\tilde{k}(\xi)$



“Real-time” imaging? (2ns FWHM)



back project



back project with $\tilde{k}(\xi)$



Summary

- Data redundancy allows reconstruction adaptive to local data statistics
 - Do iterative algorithms achieve this automatically?
- Improved timing resolution may also improve scatter rejection
 - Tradeoffs in timing and energy resolutions?
 - Algorithms to exploit the advantages of superior timing resolution
- “Real-time” imaging possible
 - Practical value?



FBP reconstruction

